ISSN 0016-7029, Geochemistry International, 2006, Vol. 44, No. 6, pp. 547–558. © Pleiades Publishing, Inc., 2006.
Original Russian Text © Yu.A. Martynov, D.W. Lee, V.V. Golozubov, S.V. Rasskazov, 2006, published in Geokhimiya, 2006, No. 6, pp. 597–609.

Geochemistry and Geodynamic Setting of Late Cretaceous–Miocene Basalts in the Southern Korean Peninsula

Yu. A. Martynov[a], D. W. Lee[b], V. V. Golozubov[a], and S. V. Rasskazov[c]

[a]*Far East Geological Institute, Far East Division, Russian Academy of Sciences, pr. Stoletiya Vladivostoka 159, Vladivostok, 690022 Russia*

e-mail: marthynov@fegi.ru

[b]*Kongju National University, College of Natural Science, Kongju, Korea*

e-mail: cdpii@knu.kongju.ac.kr

[c]*Institute of the Earth's Crust, Siberian Division, Russian Academy of Sciences, ul. Lermontova 128, Irkutsk, 664033 Russia*

Received September 15, 2004

Abstract—Newly obtained data highlight strong geological and geochemical differences between Late Cretaceous–Paleogene and Eocene–Middle Miocene volcanic rocks in the southern Korean Peninsula. The rocks are spatially separated and differ in the proportions of acid and basic varieties. The Late Cretaceous–Paleogene basalts are similar to suprasubduction rocks in having high Al_2O_3, LILE, and Th contents, and low TiO_2 and HFSE contents. The Miocene basalts have a composition intermediate between those of subduction and within-plate rocks. Compared to subduction rocks, they are lower in radiogenic Sr, K, LILE (Cs, Rb, Ba), and Th and higher in MgO, Ni, Ti, and HREE. A drastic change in U, Ba, Rb, Ce, Th, and $^{87}Sr/^{86}Sr$ in the basic volcanic rocks of the southern Korean Peninsula at the Late Cretaceous–Paleogene boundary suggests a decreasing sedimentary contribution to the magma. The latter testifies to a change in the direction of the motion of the oceanic and continental plates, increasing compressional forces and, finally, the cessation of subduction. The synthesis of the original authors and published data on Cenozoic volcanism of the southern Korean Peninsula and the eastern Sikhote Alin showed that the tectonic evolution of the eastern Eurasian margin occurred in four stages: Late Cretaceous–Paleogene, Eocene–Oligocene, Early, and Middle-Miocene.

DOI: 10.1134/S0016702906060024

INTRODUCTION

The tectonic evolution of the Eurasian continental margin in the Cenozoic resulted in the opening of the Sea of Japan and the formation of the modern Japanes island-arc system. Most geologists suggest that these events were initiated in the Middle–Late Miocene (20–12 Ma) [1, 2] and were caused by back-arc spreading, subduction roll-back toward the deep-water trench, and the upwelling of a depleted asthenospheric diapir in the extensional zone. When large-scale extension ceased (in the Late Cenozoic, at 10–3 Ma), numerous basaltic plateau were generated in the Sikhote Alin, northeastern China, Korea, and southwestern Japan.

This model is inconsistent with data obtained in the past decade on Late Cretaceous–Cenozoic volcanogenic sequences in the southern part of the Russian Far East. The eastern Eurasian margin presumably experienced more a complex and a longer term of tectonic evolution. Basaltic sequences of this area have been formed since at least the Eocene, after the cessation of subduction, during the initial stage of rifting [3, 4] caused by the activation of transform faults, slab break off with the opening of slab windows [5]. This conclusion is confirmed by our geological data, which were obtained during field and laboratory investigations of Late Cretaceous–Miocene basaltic volcanism in the southern Korean Peninsula.

BRIEF GEOLOGICAL CHARACTERISTICS OF THE MESO–CENOZOIC VOLCANOGENIC ROCKS OF THE KOREAN PENINSULA

Starting in the Middle Jurassic (180–155 Ma), after collision between the Syno-Korean, Soboekson–Hinda, and Honshu continental blocks, the Korean Peninsula existed as a stable craton unaffected by significant rotation or spatial displacements [1, 6, etc.]. Most of the peninsula belongs to the Sino–Korean paraplatform, and only northeastern and northwestern portions belong to the Sikhote Alin and cat-Asian fold systems [7].

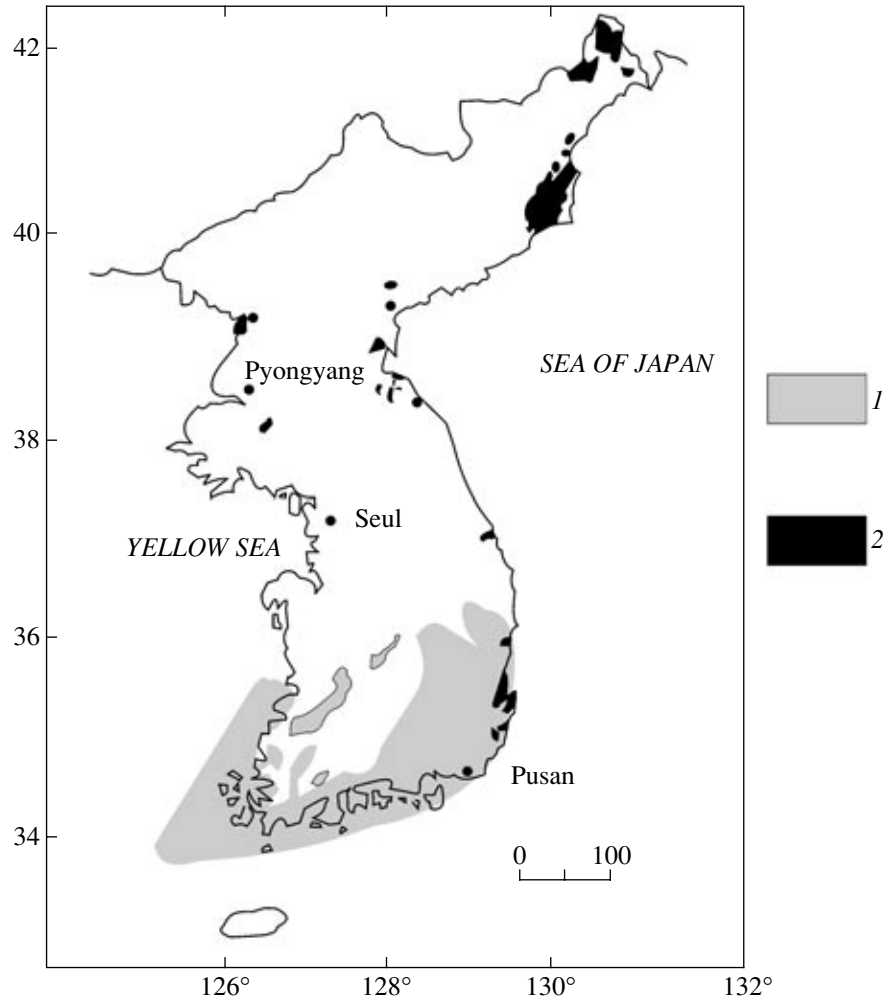

Fig. 1. Location scheme of the Late Cretaceous (*1*) and Paleogene–Miocene (*2*) volcanic rocks of Korea (modified after [7]).

Volcanic activity in the study area can be traced from the Late Jurassic (about 135 Ma), when the subduction of the Kula plate produced the Late Jurassic–Early Cretaceous volcanic belt of North Korea. In the Late Cretaceous, the subduction of the Pacific plate produced the Southern Korean–Japan volcanic belt, a chain of marginal–continental volcanic belts extending along the eastern Asian continental margin, in the southern Korean Peninsula (Fig. 1). The K–Ar age of the volcanic rocks varies from 79 to 57 Ma, with a southward decrease in the age of the volcanic centers [7]. The lower portions of the volcanic sequences are made up of the basaltic lavas and agglomerate tuffs, which are underlain and overlain by tuffogenic mudstones [7]. They are subsequently replaced upsection by basalts and basaltic andesites, basaltic volcanogenic conglomerates, and basic agglomerate tuffs. The sequence is crowned by andesites, dacites, and rhyolites. The total thickness of the Late Cretaceous–Paleogene volcanogenic rocks of the depression is estimated at 2000 m [8], with acid volcanic rocks accounting for 1000–1500 m. The basic to acid evolution and a the large volume of the acid units are typical features of Late Cretaceous volcanism in the southern part of the Korean Peninsula and the Eastern Sikhote Alin volcanic field north of it.

The Eocene–Miocene, mainly basic volcanic rocks occur as isolated fields in the rear part of the Late Cretaceous–Paleogene volcanic front, in the southern part of the peninsula (Fig. 1). Rocks of the middle Eocene volcanic stage (46–44 Ma) occurred only locally. In the Pohang depression, this stage produced basaltic flows and NE-trending basic dikes [8]. This stage was followed by an interlude in magmatic activity, which ended early in the Miocene. The Miocene volcanic rocks, which also occur mostly within the Pohang depression, are composed of 23- to 21-Ma extrusive andesites and dacite flows intercalating with continental clastic rocks [9]. They are overlain by marine and continental sediments with scarce flows of acid and basic lavas. The K–Ar age of the basaltic magmas is 21–18 Ma. The sequence is capped by the marine sedi-

mentary rocks, which are overlain by basalts with an age of 13.6–15.2 Ma and cut by felsitic dikes [10].

METHODS

Major elements were analyzed by conventional chemical techniques at the Laboratory of the Geological Institute, Far East Division, Russian Academy of Sciences (analyst L.V. Shkodyuk). Trace elements were analyzed by ICP-MS, and the age of the rocks was determined by the K–Ar method at the Laboratory of Isotopic Studies and Geochronology at the Institute of the Earth's Crust, Siberian Division, Russian Academy of Sciences. The chemical preparation of samples for trace-element and isotope analysis was conducted with the use of doubly distilled water from deep levels of Lake Baikal. Acids of high-purity-grade doubly purified by isothermal distillation were used for the sample preparation. HF was purified in a Teflon apparatus, while water, HNO_3, and HCl were purified in a quartz apparatus. The ICP-MS analysis was conducted on a VG Plasmaquad PQ2+ at the Irkutsk Center of Collective Use. The apparatus was calibrated on the BHVO-1, AGV-1, and BIR-1 international standards and the U-94-5 (basanite) internal laboratory standard. Strontium isotope ratios were analyzed on a Finnigan MAT 262 mass spectrometer at the Irkutsk Center of Collective Use. The average $^{87}Sr/^{86}Sr$ values of the NBS SRM 987 isotope standard and the JB-2 rock standard were 0.71028 ± 0.00002 and 0.70372 ± 0.00002, respectively. The K–Ar age of the volcanic rocks was determined on a MI-1201 mass spectrometer modified for the simultaneous measurement of Ar^{36} and Ar^{40} with isotope dilution by air Ar. The K contents were determined in three aliquots by flame photometry with measurement errors of no more that 1.5%. The total error in K–Ar determinations involved instrumental errors in the determinations of K and radiogenic Ar.

GEOCHEMISTRY OF LATE CRETACEOUS–MIOCENE BASALTS

The Late Cretaceous–Paleogene basic volcanic rocks are classed with the high-K and moderate-K series (Fig. 2). Geochemically, they are typical suprasubduction rocks with high Al, LILE, and Th and low TiO_2 and HFSE contents (Fig. 3). In discriminant diagrams, the data points of Late Cretaceous–Paleogene rocks plot in the fields of modern island-arc basalts (Fig. 4).

Due to their limited abundance, the Early Eocene volcanic rocks are poorly studied. Compared to Late Cretaceous–Paleogene subduction basalts, they have lower contents of radiogenic Sr (Fig. 5).

The Miocene basalts distinctly differ in geochemistry from the earlier subduction basalts. In addition to low contents of radiogenic Sr (Fig. 5), the Early Eocene basalts have relatively low alkalinity (Fig. 2) and low abundances of LILE (Cs, Rb, Ba) and Th, at elevated contents of MgO, Ni, Ti, and HREE (Fig. 3). In terms of geological–geochemical characteristics, these rocks approximate the Eocene–Oligocene lavas of the Eastern Sikhote Alin [3, 4], which formed during the initial stage of slab break off by transform faults with the formation of slab windows.

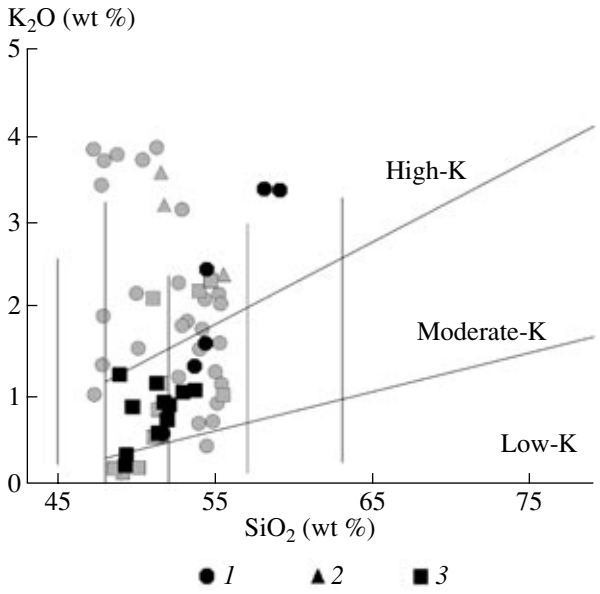

Fig. 2. K_2O–SiO_2 classification diagrams for basic volcanic rocks from the southern Korean Peninsula. (*1*) Late Cretaceous–Paleogene; (*2*) Early Eocene; (*3*) Miocene. Filled symbols are the original data; gray symbols are from [6, 8–15] data.

PETROGENESIS

In accordance with the Miocene model for the opening of the Sea of Japan, all pre-Miocene magmatic rocks of the southern Korean Peninsula are thought to be related to the subduction of the Pacific plate beneath the Asian continental margin, while the younger rocks are interpreted as produced by post-subduction rifting [8]. The rift-related rocks include the Miocene lavas formed during the opening of the Sea of Japan and the Pliocene–Quaternary lavas.

Our data showed that only the Late Cretaceous–Paleogene volcanic rocks of the southern Korean Peninsula (79–57 Ma) are typical subduction rocks. They compose the Southern Korean–Japan volcanic belt and geochemically resemble modern island-arc basalts.

Since the Eocene time, the character of volcanism in the southern Korean Peninsula has significantly changed. The acid lavas strongly decreased in volume,

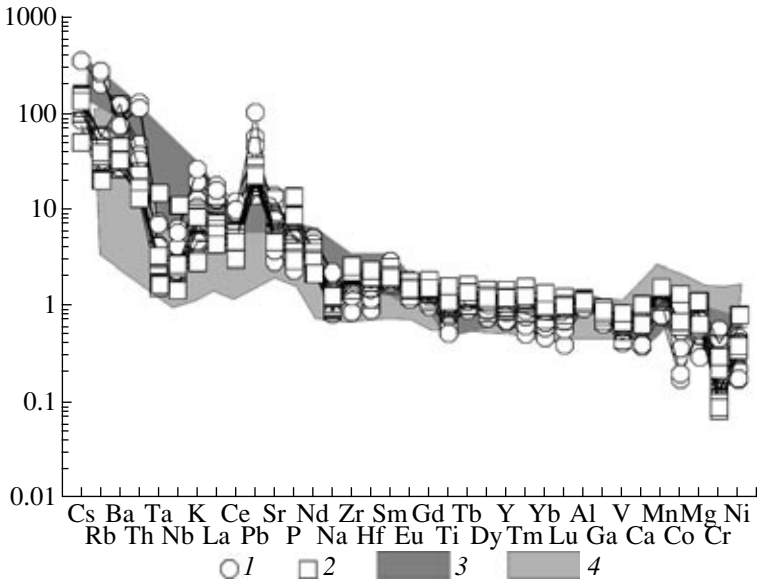

Fig. 3. MORB-normalized major and trace-element abundances. Normalizing values are from [16]. (*1*) Late Cretaceous–Paleogene; (*2*) Miocene; (*3, 4*) published [6, 8–15] analytical data on Late Cretaceous–Paleogene (*3*) and Miocene (*4*) basalts.

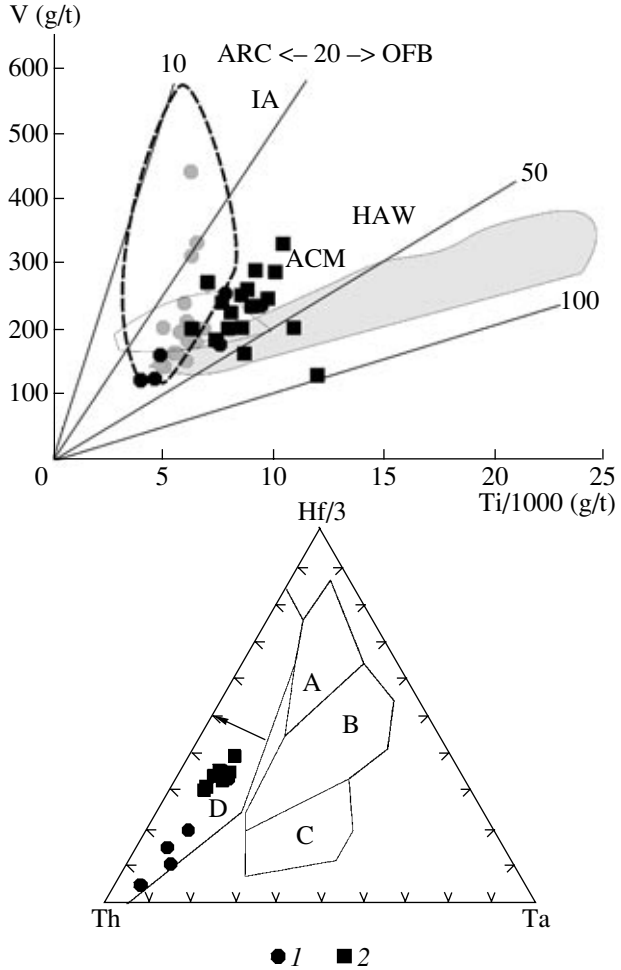

Fig. 4. Ti–V [17] and Th–Hf–Ta [18] (with our modifications) classification diagrams for Late Cretaceous–Cenozoic basalts of the southern Korean Peninsula. Symbols are shown in Fig. 2. Basaltic fields in the Ti–V diagram: (IA) island arc, (HAW) Hawaiian islands; Basaltic fields in the Th–Hf–Ta diagram: (A) mid-oceanic ridges, (B) mid-ocean ridges and within-plate basalts, (C) within-plate basalts, (D) island arcs and active continental margin basalts. Data are from [6, 8–15].

Major (wt %) and trace (g/t) element abundances in representative samples of basic volcanic rocks of the southern Korean Peninsula

Component	ky-10-00	ky-12-00	ky-13-00	ky-14-00	ky-20-00	ky-21-00	ky-23-00	ky-1-00	ky-2-00
	Number								
	1	2	3	4	5	6	8	12	13
	Age (Ma)								
	82*	82*	82*	78.50				19*	19*
SiO_2	58.98	53.44	58.77	57.22	50.17	63.68	51.67	50.20	49.73
TiO_2	0.60	0.80	0.70	0.86	1.27	0.69	1.52	1.40	1.20
Al_2O_3	16.56	17.50	17.70	17.36	18.69	15.69	18.49	18.24	18.81
Fe_2O_3	4.49	5.28	4.02	5.86	3.65	4.79	9.06	2.00	6.25
FeO	0.57	3.46	1.52	1.59	5.00	1.70	1.91	3.95	0.08
MnO	0.13	0.10	0.06	0.12	0.19	0.08	0.13	0.15	0.16
MgO	2.92	4.22	3.10	2.01	5.25	0.53	2.13	4.64	5.91
CaO	7.15	8.11	5.84	8.54	9.37	2.69	4.71	11.78	11.98
Na_2O	3.08	3.02	4.10	2.53	3.11	5.14	5.89	2.84	2.46
K_2O	2.80	2.45	2.19	1.90	0.59	2.42	1.33	0.74	0.58
P_2O_5	0.64	0.33	0.33	0.30	0.19	0.15	0.34	0.95	0.28
LOI	1.62	1.46	1.11	1.10	1.55	1.91	2.34	2.17	2.08
Total	99.54	100.35	99.70	99.60	99.87	99.51	99.69	99.40	99.78
Rb	72.66	110.56	65.31	73.36	14.67	62.52	21.89	10.89	11.31
Ba	1082.38	735.52	997.92	795.37	167.11	879.94	214.72	213.75	160.51
Sr	622.22	688.20	815.83	748.87	458.10	538.10	1211.42	510.39	413.97
Pb	18.77	16.65	16.12	14.69	5.03	7.79	7.79	7.44	5.86
Ni	13.00	17.00	10.00	12.00	36.00	21.00	17.00	48.00	60.00
Co	8.00	1.40	8.00	9.00	27.00	8.00	14.00	45.00	52.00
Cr	12.00	36.00	13.00	19.00	68.00	64.00	8.00	30.00	59.00
V	140.00	160.00	150.00	210.00	250.00	110.00	230.00	160.00	180.00
Zr	159.91	97.61	141.24	157.91	127.97	58.94	91.67	159.01	122.58
Hf	4.00	3.37	3.78	4.35	3.15	1.94	3.31	3.51	3.10
La	41.76	32.17	44.39	32.50	11.70	22.76	30.77	13.46	11.35
Ce	75.19	63.33	77.72	68.74	28.78	48.36	67.30	31.24	28.05
Pr	9.07	7.17	9.87	8.68	3.71	5.20	8.17	4.35	3.72
Nd	36.51	33.25	39.69	35.57	17.64	20.87	36.47	20.77	18.08
Sm	6.62	5.54	7.81	6.97	4.46	3.80	7.33	5.00	4.72
Eu	1.75	1.42	2.07	1.67	1.38	1.02	1.87	1.54	1.44
Gd	5.39	3.59	6.78	4.40	4.54	2.96	6.03	5.33	4.90
Tb	0.78	0.60	1.03	0.76	0.74	0.43	0.84	0.81	0.83
Dy	4.30	3.37	5.37	3.78	4.83	2.19	4.39	5.00	5.04
Ho	0.85	0.64	1.11	0.70	0.96	0.42	0.83	1.03	1.06
Er	2.38	1.75	2.95	2.18	2.95	0.99	2.21	2.92	3.20
Tm	0.36	0.23	0.50	0.38	0.46	0.19	0.34	0.47	0.50
Yb	2.03	1.62	2.30	2.55	2.48	0.91	1.75	2.65	2.86
Lu	0.31	0.29	0.36	0.34	0.41	0.14	0.25	0.41	0.43
Nb	9.99	6.23	9.35	7.50	5.23	7.79	9.26	5.03	3.92
Y	29.02	18.81	37.57	26.14	33.77	11.59	23.37	32.46	29.32
Ta	0.60	0.50	0.53	0.46	0.37	0.48	0.52	0.29	0.33
Th	7.96	5.63	8.50	6.37	1.67	6.32	3.86	1.77	1.70
Sc	15.54	22.79	13.23	20.89	34.18	10.95	19.20	28.95	34.39
Ga	11.0	12.00	15.00	12.00	12.00	8.00	11.00	14.00	13.00
Cs	1.20	2.43	1.85	0.78	1.08	1.08	0.57	0.45	0.93
U	1.62	1.13	1.65	1.67	0.41	0.88	1.07	0.46	0.42
Be	2.00	1.70	2.00	1.60	1.10	1.20	1.60	1.50	0.80
B	6.00	13.00	7.00	11.00	13.00	93.00	96.00	9.00	9.00
$^{87}Sr/^{86}Sr$	–	0.7099400	–	0.7086600	–	–	–	–	–

Table (Contd.)

Component	ky-3-00	ky-4-00	ky-5-00	ky-7-00	ky-8-00	ky-9-00	ky-15-00	ky-17-00	ky-18-00
	Number								
	14	15	16	17	18	19	20	21	22
	Age (Ma)								
	19*	19*	17.00	21.00	19*	19*		19*	19*
SiO_2	48.38	59.91	47.85	50.10	50.14	49.00	50.03	52.44	51.88
TiO_2	1.30	0.70	1.96	1.46	1.30	1.04	1.78	1.40	1.40
Al_2O_3	18.79	17.06	17.40	17.09	17.39	18.22	17.16	16.54	17.78
Fe_2O_3	6.74	3.19	0.21	5.09	5.27	6.34	5.20	4.48	3.65
FeO	1.11	1.60	5.70	1.85	1.72	1.92	6.31	5.82	6.34
MnO	0.19	0.19	0.17	0.18	0.14	0.16	0.20	0.20	0.20
MgO	5.44	3.21	8.41	5.92	5.93	5.54	4.33	4.55	4.77
CaO	12.04	6.70	11.98	11.64	11.36	12.61	8.47	8.01	7.62
Na_2O	4.00	4.13	2.58	2.50	2.31	2.70	3.22	3.36	3.46
K_2O	0.36	1.96	1.26	0.94	0.90	0.90	1.16	1.08	1.06
P_2O_5	0.38	0.46	0.35	0.59	0.35	0.62	0.26	0.22	0.21
LOI	0.82	0.44	2.40	2.10	2.65	0.98	1.49	1.12	1.16
Total	99.55	99.63	99.77	99.60	99.94	100.15	99.97	99.55	99.92
Rb	17.55	41.24	31.13	32.22	24.09	14.28	19.51	23.74	21.42
Ba	160.52	385.50	775.00	277.49	259.65	190.27	277.26	203.21	200.31
Sr	469.96	432.89	1138.04	474.59	407.06	511.55	433.60	414.23	402.42
Pb	5.61	13.80	4.09	7.22	7.07	5.53	8.31	6.94	6.59
Ni	40.00	12.00	80.00	30.00	31.00	33.00	34.00	34.00	38.00
Co	32.00	11.00	37.00	40.00	44.00	33.00	38.00	24.00	27.00
Cr	35.00	10.00	110.00	44.00	37.00	22.00	27.00	59.00	80.00
V	200.00	91.00	130.00	230.00	220.00	200.00	200.00	200.00	250.00
Zr	150.90	111.09	183.33	153.08	154.38	107.57	162.57	164.45	165.08
Hf	3.93	2.84	4.53	4.57	3.50	2.39	4.06	4.06	4.00
La	13.65	20.14	22.26	18.02	15.18	10.54	17.38	15.40	13.67
Ce	31.95	43.58	43.63	41.67	34.90	23.93	41.86	37.28	33.91
Pr	4.82	5.70	4.96	4.79	4.73	3.32	5.47	4.71	4.30
Nd	24.06	25.91	24.69	27.80	22.07	15.68	25.51	22.04	20.62
Sm	5.87	5.53	5.57	6.02	5.57	4.24	6.44	5.36	5.14
Eu	1.64	1.57	1.73	1.56	1.64	1.27	1.82	1.58	1.52
Gd	5.30	5.53	3.98	5.84	5.75	4.26	6.79	5.49	5.61
Tb	0.94	0.86	0.66	1.04	0.93	0.67	1.10	0.92	0.92
Dy	5.70	5.41	3.77	5.76	5.75	4.13	6.64	5.78	5.50
Ho	1.12	1.04	0.78	1.11	1.16	0.84	1.39	1.18	1.18
Er	3.18	2.89	2.08	3.65	3.39	2.40	3.95	3.59	3.29
Tm	0.52	0.46	0.38	0.62	0.53	0.38	0.71	0.57	0.57
Yb	3.67	2.42	2.17	4.06	3.10	2.17	3.61	3.10	3.01
Lu	0.54	0.34	0.36	0.50	0.47	0.32	0.56	0.47	0.45
Nb	5.08	7.20	24.80	4.90	5.27	3.41	5.78	6.25	6.17
Y	29.86	32.92	24.39	35.92	36.01	26.65	40.57	34.28	33.77
Ta	0.33	0.47	1.87	0.35	0.28	0.20	0.34	0.40	0.42
Th	1.61	3.36	2.92	2.49	2.21	1.51	2.68	2.04	1.96
Sc	38.02	18.50	28.97	43.17	43.49	38.87	38.73	34.03	33.16
Ga	12.00	13.00	14.00	14.00	15.00	11.00	15.00	13.00	14.00
Cs	0.86	2.43	1.07	1.09	0.68	0.52	0.34	1.03	0.92
U	0.38	1.24	0.77	0.51	0.49	0.35	0.64	0.50	0.53
Be	0.80	1.60	1.20	1.20	1.30	0.90	1.30	1.20	1.20
B	16.00	6.00	12.00	17.00	18.00	10.00	12.00	17.00	27.00
$^{87}Sr/^{86}Sr$	0.7042900	–	–	0.7043800	–	–	–	–	–

* Age of the volcanic complex in the sampling site according to literature data.

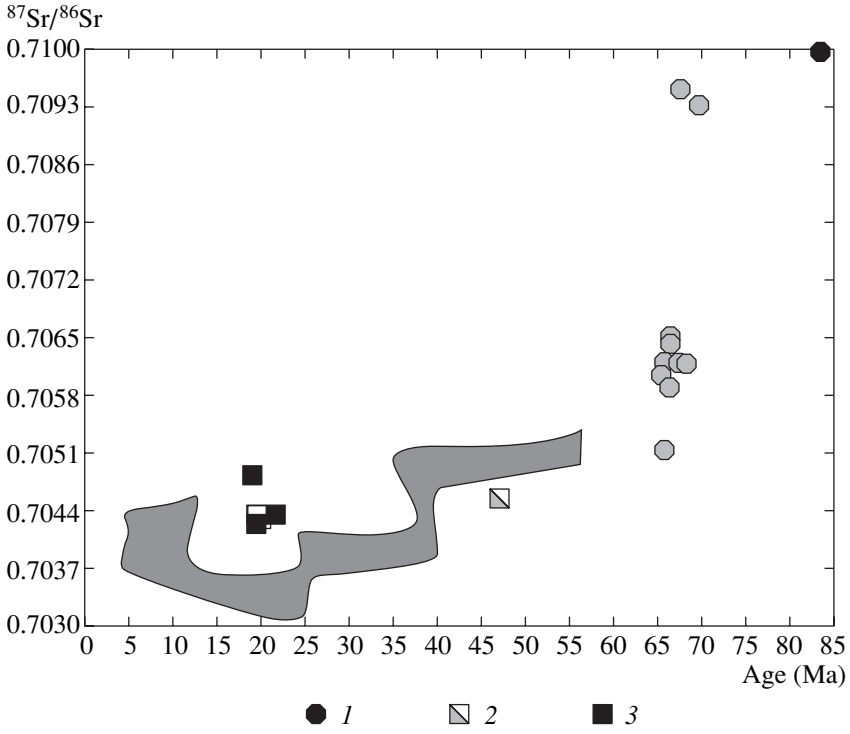

Fig. 5. Sr isotope variations in the Late Cretaceous–Cenozoic basalts of the southern Korean Peninsula depending on the eruption time. Symbols are as in Fig. 2. Filled field outlines the compositions of Cenozoic high-Al and within-plate basalts of the Eastern Sikhote Alin after [3, 4]. Data are from [8, 9, 15].

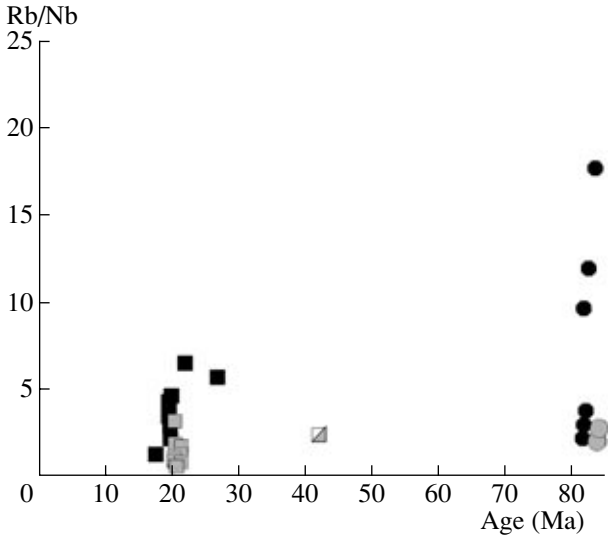

Fig. 6. Variations in the Rb/Nb ratios in the Late Cretaceous–Cenozoic basalts of the southern Korean Peninsula depending on the eruption time. Symbols are as in Fig. 2. Data are from [6, 8–15].

while active volcanic centers displaced north and northeastward, to the coast of the Sea of Japan. In addition, the isotope–geochemical characteristics of the basic volcanic rocks also changed, indicating, in combination with other data, a change in the geodynamic regime.

The Late Cretaceous–Cenozoic basaltic volcanism of the eastern Eurasian margin displays an abrupt change in isotope–geochemical characteristics within a relatively narrow time interval. Regardless of their origin mechanisms, such "geochemical jumps," record variations in the magma generation conditions, and,

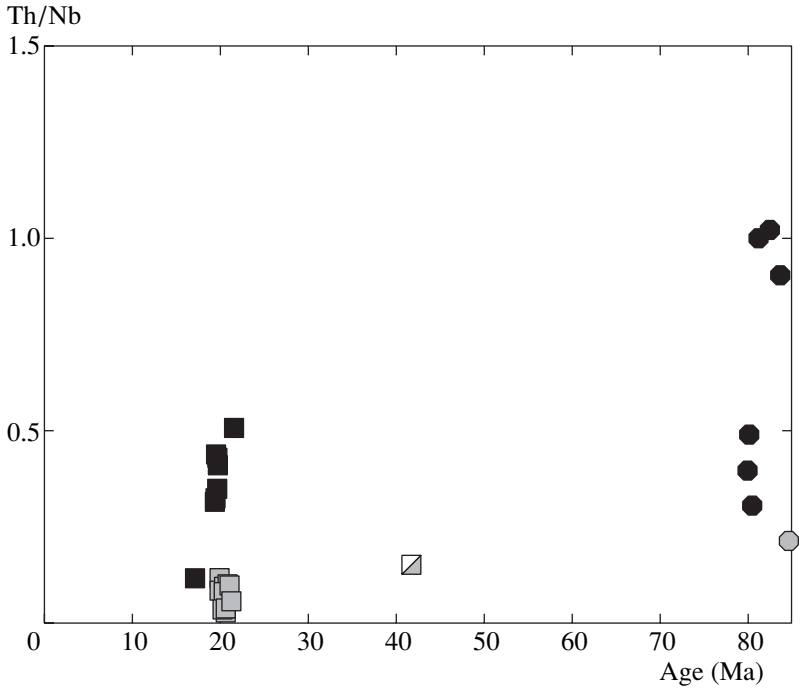

Fig. 7. Variations in the Th/Nb ratio in the Late Cretaceous–Cenozoic basalts of the southern Korean Peninsula depending on the eruption time. Symbols are as in Fig. 2. Data are taken from [6, 8–15].

hence, the dynamics of the interaction of the ocean and continental lithosphere in a continent–ocean transitional zone. The first geochemical jump, expressed as a drastic decrease in the contents of Rb, Ba, and Th (table) and the Rb/Nb (Fig. 6), Th/Nb (Fig. 7), and $^{87}Sr/^{86}Sr$ (Fig. 5) ratios, was detected in the Late Cretaceous–Paleogene basalts. The geochemical variations in lavas are related mainly to a decrease in the subduction component (Fig. 8). The latter includes elements (1) highly mobile in an aqueous magmatic fluid (U, Ba, Rb) and (2) inert (Ce, Th, ^{87}Sr). Inert components play a decisive role in the change in the geochemical composition of the volcanic rocks (Figs. 9, 10, 11, 12). Given the fact that the content of inert subduction components is controlled mainly by the amount of involved sedimentary material [20], the Late Cretaceous–Paleogene boundary marks a change in the movement direction of the oceanic and continental plates with increasing compressional stresses in the interaction zone and the subsequent cessation of subduction.

The change in the geodynamic setting of the eastern Eurasian margin in the Late Cretaceous or at the Late Cretaceous–Paleogene boundary is confirmed by numerous geological data. The onset of structural restyling in eastern and northeastern China corresponds to the Paleogene. The Eocene was marked by the activation of the ancient fault zone and the generation of new SW-trending strike-slip faults, which were accompanied by the formation of the strike-slip pull-apart sedimentation basins and intense within-plate basaltic volcanism [21]. The tectonic events were interpreted as activated by the collision of the Indian plate and changes in the convergent movements of the Pacific oceanic plate. The change in the character and localization of volcanic activity in the Korean Peninsula and eastern Sikhote Alin occurred at the Late Cretaceous–Paleogene boundary. In particular, the Early Paleogene volcanic rocks of the Bogopol Complex in the eastern Sikhote Alin (59.68–52.92 Ma) fill a superimposed depression in the rear zone of the Cretaceous volcanic belt, and formed under highly reduced conditions, which are not typical of subduction-related volcanic rocks [22].

The subsequent sudden change in the isotope–geochemical composition (Fig. 5) was recorded in the 40- to 35-Ma high-Al basalts of the eastern Sikhote Alin [3, 4].This period was marked by the formation of coal fields (Artemovsk–Tavrichsn, Luchegorsk, and others) [23] and the peak of volcanic activity related to the outpouring of the main volume of the basaltic lavas with characteristics transitional between subduction-related and within-plate basalts [3, 4]. This indicates that Eocene–Oligocene drastic change in the geochemical composition of the volcanic rocks was related to the activation of transform faults, break off of the ancient slab, formation of subduction windows, and upwelling of the depleted asthenospheric mantle into the subcontinental lithosphere.

The change in the isotope–geochemical composition of basaltic lavas of the eastern Sikhote Alin within

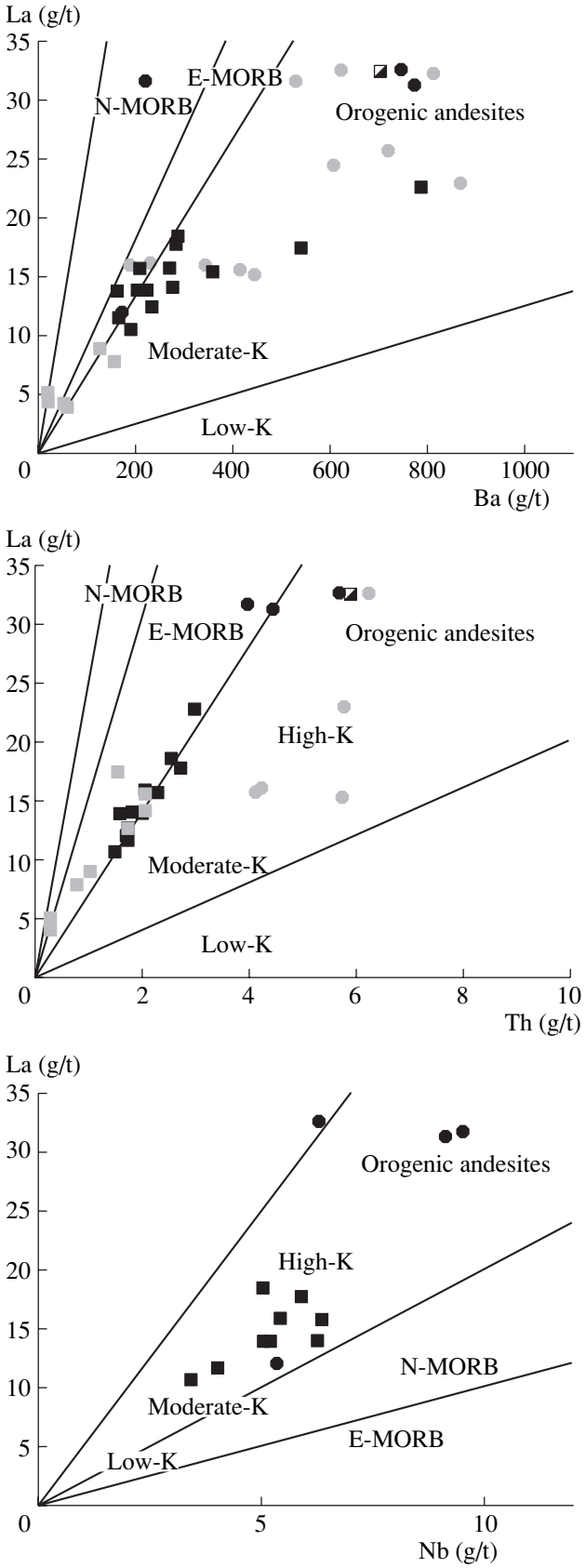

Fig. 8. La–Ba, La–Th, La–Nb [19] classification diagrams for the Late Cretaceous–Cenozoic basalts of the southern Korean Peninsula. Symbols are as in Fig. 2. Data are from [6, 8–15].

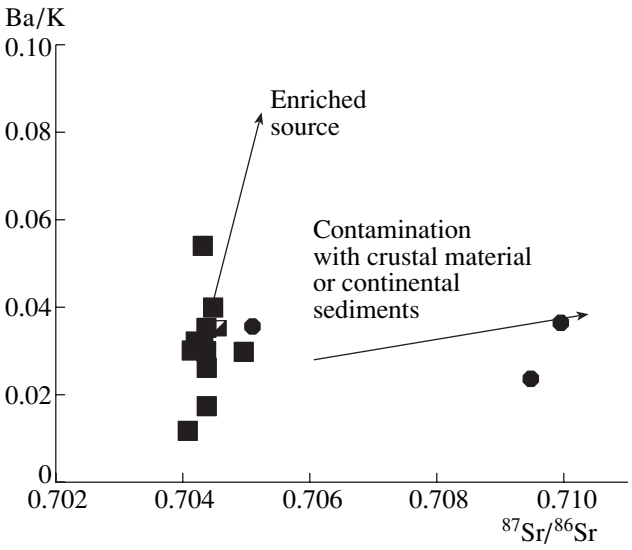

Fig. 9. Ba/K–$^{87}Sr/^{86}Sr$ [20] lkz diagram for the Late Cretaceous–Cenozoic basalts of the southern Korean Peninsula. Symbols are as in Fig. 2. Data are from [8].

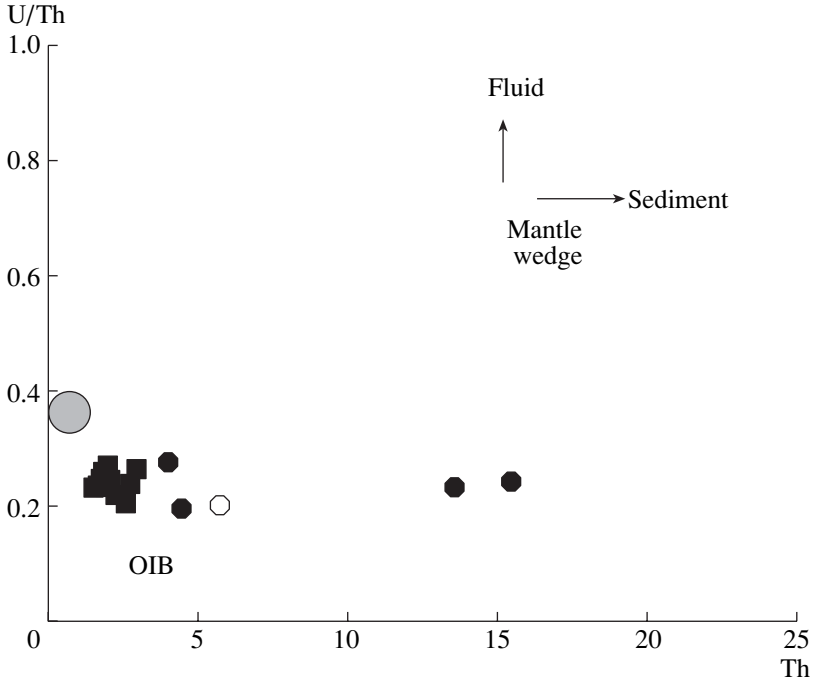

Fig. 10. U/Th–Th diagram [20] for the Late Cretaceous–Cenozoic basalts of the southern Korean Peninsula. Symbols as in Fig. 2.

25–23 Ma (Fig. 5) corresponds to the sharp activation of movements along the Hokkaido–Sakhalin and Tsusima marginal continental dextral strike-slip systems with the formation of pull-apart basins, including the deep-water basins of the Sea of Japan [24, 25, 26, etc.].

The youngest geochemical jump expressed as a sharp decrease in the concentration of radiogenic Sr ($^{87}Sr/^{86}Sr$ ratio changes from 0.7041–0.7055 to 0.7040–0.7029) was identified in the 14- to 17-Ma basalts of the rear zones of Japan [27, 2, etc.]. It is interpreted as a result of the upwelling of the depleted asthenospheric mantle into the subcontinental lithosphere during the final opening stage of the Sea of Japan, which was caused by the rotation of blocks of the paleo-Japan, separated from Eurasia [28].

Thus, a synthesis of new data with published information testifies to the occurrence of at least four geodynamic stages at the eastern margin of Eurasia. The old-

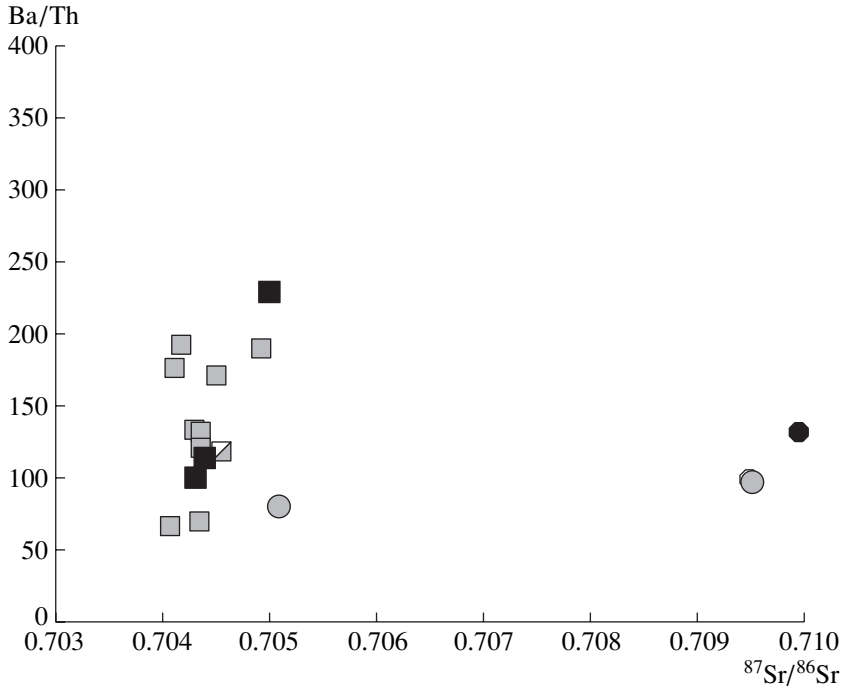

Fig. 11. Ba/Th–$^{87}Sr/^{86}Sr$ diagram [20] for the Late Cretaceous–Cenozoic basalts of the southern Korean Peninsula. Symbols are as in Fig. 2.

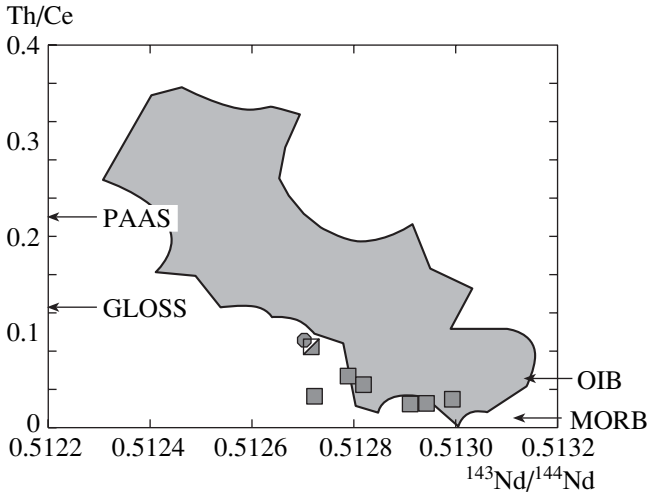

Fig. 12. Th/Ce–$^{143}Nd/^{144}Nd$ diagram [20] for the Late Cretaceous–Cenozoic basalts of the southern Korean Peninsula after literature data. Symbols are as in Fig. 2. Data are from [9].

est of them was recorded in the Late Cretaceous–Paleogene basalts of the southern Korean peninsula.

ACKNOWLEDGMENTS

This study was supported by the Russian Foundation for Basic Research (project nos. 03-05-65218 and 02-05-65326) and integration project of the Siberian and Far East divisions of RAS.

REFERENCES

1. Y. Otofuji, T. Matsuda, and S. Nohda, "Opening Mode of the Japan Sea Inferred from the Paleomagnetism of the Japan Arc," Nature **317**, 603–604 (1985).
2. K. Shuto, H. Kagami, and K. Yamomoto, "Temporal Variation of Sr Isotopic Compositions of the Cretaceous to Tertiary Volcanic Rocks from the Okushiri Island, Northeast Japan Sea," J. Min. Pet. Econ. Geol. **87**, 165–173 (1992).

3. Yu. A. Martynov, *Geochemistry of Basalts in Active Continental Margins and Mature Island Arcs; Evidence from Northwestern Pacific* (Dal'nauka, Vladivostok, 1999), [in Russian].
4. Yu. A. Martynov, "High-Alumina Basaltic Volcanism of the Eastern Sikhote Alin: Petrology and Geodynamics," Petrologiya **7** (1), 58–79 (1999) [Petrology **7** (1), 53 (1999)].
5. A. I. Khanchuk, V. V. Golozubov, Yu. A. Martynov, and V. P. Simanenko, "Early Cretaceous and Paleogene Transform Continental Margins (Californian Type) of Russian Far East," in *Tectonics of Asia* (GEOS, Moscow, 1997), pp. 240–243 [in Russian].
6. A. V. Fedorchuk and N. I. Filatova, "Cenozoic Magmatism of North Korea," Petrologiya **1**, 645–656 (1993).
7. *Geology of Korea* (Keohak-Sa Publishing, Seoul, 1987).
8. A. Pouclet, J.-S. Lee, P. Vidal, et al., "Cretaceous to Cenozoic Volcanism in South Korea and in the Sea of Japan: Magmatic Constraints on the Opening of the Back-Arc Basin," in *Volcanism Associated with Extension at Consuming Plate Margins*, Ed. by J. L. Smellie, Geol. Soc. Spec. Publ. London, No. 81, 169–191 (1995).
9. M. Shimazu, S. Yoon, and M. Tateishi, "Tectonic and Volcanism in the Sado-Pohang Belt from 20 to 14 Ma and Opening of the Yamato Basin of the Japan Sea," J. South Am. Earth Sci. **181**, 321–330 (1990).
10. S. Song and H. Lee, "Petrogenesis of Tertiary Volcanic Rocks from the Southeastern Part of Korea," in *Proceedings of the First International Symposium on Tectonic Evolution of Eastern Asian Continent, Geol. Soc. Korea 50th Anniv., Seoul, Korea, 1997* Ed. by Y. I. Lee and J. H. Kim (Seoul, 1997), pp. 219–224.
11. S. K. Hwang and S. W. Kim, "Petrology of Cretaceous Volcanic Rocks in the Milyang–Yangsan Area, Korea: Petrotectonic Setting," J. Geol. Soc. Korea **30**, 229–241 (1994).
12. K. H. Kim and J. S. Lee, "Petrochemical Studies of the Cretaceous Volcanic Rocks from the Kyeongsang Sedimentary Basin," J. Geol. Soc. Korea **29**, 84–96 (1993).
13. C. S. Kim, S. H. Yun, and C. S. Cheong, "Volcanic Stratigraphy and Petrology of the Cretaceous Volcaninc Rocks in the Mt. Sinbul-Youngchui Area, Korea," J. Geol. Soc. Korea **34**, 137–153 (1998).
14. C. K. Won, M. W. Lee, and J. M. Lee, "A Study on the Cretaceous Volcanic Activity of the Bupseongpo Area," J. Geol. Soc. Korea **27**, 416–433 (1991).
15. S. H. Yun, "Strontium Isotope Composition and Petrochemistry of the Cretaceous Chaeyaksan Volcanics, Northern Yucheon Volcanic Field, South Korea," J. Geol. Soc. Korea **34**, 161–171 (1998).
16. J. A. Pearce and I. J. Parkinson, "Trace Element Model for Mantle Melting: Application to Volcanic Arc Petrogenesis," in *Magmatic Processes and Plate Tectonics*, Geol. Soc. London Spec. Publ. **76**, 373–403 (1993).
17. I. W. Shervais, "Ti–V Plots and the Petrogenesis of Modern and Ophiolitic Lavas," Earth. Planet Sci. Lett. **59** (1), 101–118 (1982).
18. D. A. Wood, "The Application of Th–Hf–Ta Diagrams to Problem of Tectonomagmatic Classification and to Establishing the Nature of Crustal Contamination of Basaltic Lavas of the British Tertiary Volcanic Province," Geotektonika **50**, 11–30 (1980).
19. J. B. Gill, *Orogenic Andesites and Plate Tectonics* (Springer, Berlin, 1981).
20. C. Hawkesworth, S. Turner, D. Peate, et al., "Elemental U and Th Variations in Island Arc Rocks: Implications for U-Series Isotopes," Chem. Geol. **139**, 207–221 (1997).
21. Q. Fan and P. R. Hooper, "The Cenozoic Basaltic Rocks of Eastern China: Petrology and Chemical Composition," J. Petrol. **32** (4), 765–810 (1991).
22. A. V. Grebennikov, "The Ignimbrites of Yakutinskaya Volcanic Depression, Primorye, Russia," in *Proceedings of International Field Conference on Anatomy and Textures of Ore-Bearing Granitoids of Sikhote Alin (Primorye Region, Russia) and Related Mineralisation, Vladivostok, Russia, 1998,* Ed. by R. Seltmann, G. Gonevchuk, and A. Khancuk (GFZ Press, Potsdam, 1998), pp. 25–31.
23. B. I. Pavlyutkin and T. I. Petrenko, "Stratigraphy of the Tertiary Deposits of the Southeastern Margin of the Khankai Massif," Tikhookean. Geol., No. 2, 18–28 (1994).
24. S. Lallemand and L. Jolvet, "Japan Sea: Pull-Apart Basin?," Earth Planet. Sci. Lett. **76**, 375–389 (1986).
25. K. K.Tamaki, J. Suyhiro, J. C. Allen, and K. Pisciotto, in "Tectonic Synthesis Is and Implications of Japan Sea ODR Drilling," Proc. Ocean Drill. Program: Sci. Res. **127–128** (2), 1333–1348 (1992).
26. S. H. Yoon and S. K. Chough, "Regional Strike-Slip in the Eastern Continental Margin of Korea and Its Tectonic Implications for the Evolution of Ulleung Basin, East Sea (Sea of Japan)," Geol. Soc. Am. Bull. **107** (1), 83–97 (1995).
27. S. Nohda, Y. Tatsumi, Y. Otofuji, et al., "Asthenospheric Injection and Back-Arc Opening: Isotopic Evidence from Northeast Japan," Chem. Geol. **68**, 317–327 (1988).
28. Y. Otofuji, "Large Tectonic Movement of the Japan Arc in Late Cenozoic Times Inferred from Paleomagnetism: Review and Synthesis," The Island Arc. **5**, 229–249, (1996).